A Standard Addition Technique To Quantify Photoacid Generation in Chemically Amplified Photoresist

Adam R. Pawloski, Christian, and Paul F. Nealey*

Center for Nanotechnology and Department of Chemical Engineering, University of Wisconsin, Madison, Wisconsin 53706

Received May 29, 2001. Revised Manuscript Received August 7, 2001

A technique to determine the efficiency of the decomposition of photoacid generators to produce photoacid and the concentration of acid necessary to image chemically amplified photoresists was designed, implemented, and validated. The technique is analogous to a standard addition experiment; known concentrations of a base quencher are added to a series of otherwise identical resist formulations. To produce the same free acid concentration within the resist films after neutralization, the concentration of photogenerated acid must increase by an amount equal to the known concentration of added base. The increase in exposure dose required to create this additional acid is indirectly determined as a function of base loading using resist dissolution behavior (contrast curves). The main assumptions implicit in the model to extract the Dill *C* parameter (a parameter proportional to the quantum yield) from experiments were validated using X-ray exposure and a positive tone photoresist system consisting of poly(*p*-*t*-butoxycarbonyloxystyrene-*co*-*p*-hydroxystyrene) as the base resin, norbornene dicarboximidyl triflate as the photoacid generator, and 1-piperidineethanol as the base quencher. Resin deprotection monitored by FTIR and dissolution rate measurements provided independent evidence that the bulk dissolution rate, the dissolution induction time, and the extent of deprotection as a function of the free acid concentration remained the same for resists with and without base.

Introduction

Lithographic patterning is the limiting techology for semiconductor device manufacturing. Since the 1970s, the resolution of optical lithography has continuously improved. The smallest printable feature into photoresist by an optical exposure system is directly proportional to the wavelength of light used in the exposure tool.[1] The primary means of improving pattern resolution has been to decrease the wavelength of the exposure source. Features with quarter micron dimensions, for example, can be patterned using 365 nm (I-line) tools. Devices with critical dimensions less than 150 nm are now printed with state-of-the-art tools using 193 nm light.[2] As a consequence of moving to shorter wavelength radiation, photoresist materials must be redesigned for every generation of exposure tools. One of the major challenges in the design of resist materials is the incorporation of chemical mechanisms to make them light sensitive; photochemical reactions must be accomplished at low exposure doses to produce significant changes in the resist dissolution rate. The transition from 365 to 248 nm exposure sources required the invention of a new paradigm in resist chemistry. Since early deep ultraviolet exposure sources were of low intensity, manufacturing throughput would have been severely hindered by the long exposure times required by conventional resists. The concept of chemical amplification, described below, was introduced to increase sensitivity.[3,4] The majority of all advanced resist materials for future generations of optical lithography at 193 and 157 nm are based on chemical amplification. Likewise, chemically amplified resist technology is readily applied to so-called next generation lithography, in which the exposure sources are high-energy, ionizing forms of radiation, such as electron beams, X-rays, and extreme ultraviolet radiation.

The general chemical mechanisms of chemical amplification within resist films are identical for all forms of exposure. A chemically amplified resist contains a photoacid generator (PAG) dispersed within a polymeric resin. Upon exposure to some form of radiation, an acid catalyst is created by photolysis or radiolysis of the PAG. By heating the film during a postexposure bake (PEB), the acid diffuses through the matrix resin and catalyzes reactions that ultimately alter the dissolution properties of the exposed regions. In the case of positive tone resists examined in this work, the acid catalyst acts to remove protecting groups from the backbone of the resin polymer, changing its chemistry and increasing its dissolution rate in a developer solution. The dissolution rate is a highly nonlinear function of the extent of deprotection. Amplification is derived from the fact that each molecule of acid catalyzes many reactions. The process is extremely sensitive to radiation since only a

* Corresponding author: e-mail nealey@engr.wisc.edu.

(1) Thompson, L. F., Willson, C. G., Bowden, M. J., Eds.; *ACS Symp. Ser.* **1983**, *Vol. 219.*

(2) Association, S. I. International Technology Roadmap for Semiconductors: 2000 update, International SEMATECH, 2000.

(3) Ito, H.; Willson, C. G. *Org. Coat. Appl. Polym. Sci. Proc.* **1983**, *48*, 60−64.

(4) Ito, H.; Willson, C. G. *Polym. Eng. Sci.* **1983**, *23,* 1012−1018.

10.1021/cm010529a CCC: $20.00
Published on Web 10/09/2001

very small concentration of acid must be generated by exposure, and PAG molecules that efficiently produce acid upon exposure are selected for the resist. The extent of chemical change to the resin polymer is controlled by the time and temperature of the PEB. The difference in the dissolution rates of the exposed and unexposed regions is then exploited during development to produce resist patterns.

Common PAGs, like sulfonium and iodonium salts, have been formulated with many different resin polymers and exposed to numerous forms of radiation (248 nm, 193 nm, 157 nm, 13.4 nm, X-ray, e-beam, etc.).[5−10] The selection of PAG affects the final resist pattern in several ways. First, the extent of conversion of PAG to acid during exposure impacts the resist sensitivity. To minimize exposure time, it is favorable to use PAGs that undergo efficient conversion to acid. Dissipation and transfer of energy in condensed media complicate the photochemical reactions in a resist film.[11,12] For a given PAG, the efficiency of the photochemical reaction depends on both the type of radiation and the chemical environment. Therefore, photoacid generation must be characterized for a given PAG/resin combination. Second, the composition of the acid generated from the PAG determines its catalytic and mass transport properties that affect the resist chemistry. Acid strength, volatility, and its diffusive behavior all affect the chemical reactions during the PEB that ultimately determine the resolution and contrast of the resist pattern.[13,14] Furthermore, the PAG may act as a dissolution inhibitor; i.e., the dissolution rate of the unexposed resist is decreased by the addition of PAG.[15] Dissolution inhibition alters the minimum and maximum dissolution rates of the resist and influences the resist contrast.

To optimize photoresist formulation and to provide essential information for modeling the image formation process, it is necessary to quantify the decomposition of photoacid generators upon exposure and the concentration of photoacid in the resist film. Techniques to measure acid concentrations directly must be extremely sensitive since the amount of acid generated at lithographic doses is very small (micromoles of acid per grams of resist). Also, film-based techniques are likewise complicated by the diminutive amount of material present in the film. Most PAGs do not exhibit a change in absorbance after exposure, eliminating spectroscopic absorption techniques as a means to monitor PAG concentration in films.[16] The most common method employed to measure the concentration of acid in exposed resist is the spectrophotometric titration of extracted resist films using an acid-sensitive indicator dye.[17−19] Calibration and measurement procedures for this method are cumbersome and require large exposed areas, a consequence that excludes the use of small field exposure systems, such as electron beams. Film-based techniques that monitor the absorbance or fluorescence of acid-sensitive dyes within resist films offer improvement over spectrophotometric titration;[20−25] however, these techniques also require extensive calibration, and fluorescence spectrophotometers are not common to many laboratories. Additionally, any film-based technique must verify that the addition of the dye does not alter the resist photochemistry in any way, whether by sensitization, increasing absorption, or the presence of side reactions.

To make quantification of photoacid generation easier and allow for comparisons across exposure platforms, we have developed a method that relies on resist dissolution as an analytical tool. The technique is based on an in situ neutralization of photogenerated acid by a base quencher that is added to the resist formulation. Analogous to a standard addition experiment, a series of resist solutions are prepared with compositions differing only in the concentration of the base additive. The addition of base to the resist neutralizes a stoichiometric quantity of acid generated during exposure. Increasing the concentration of base increases the exposure dose necessary to generate additional acid to overcome neutralization and obtain an equivalent concentration of free acid within the film. Under conditions where the free acid concentration is the same for each resist film, the dissolution rate of the film is assumed to remain constant if all processing conditions are identical (post-apply bake, PEB, film thickness, development time, etc.). This allows resist dissolution to be used as a type of analytical detector for determining states of an equivalent free acid concentration. Under such conditions we have developed a model to predict the Dill *C* parameter (a parameter that is proportional to the quantum yield) for photoacid generation. Once the *C* parameter has been determined, the concentration of

(5) Pawlowski, G.; Dammel, R.; Przybilla, K. J.; Roeschert, H.; Spiess, W. *J. Photopolym. Sci. Technol.* **1991**, *4*, 389−402.
(6) Hong, X. Y.; Feng, H. B. *J. Photopolym. Sci. Technol.* **1990**, *3*, 327−334.
(7) Schwartzkopf, G.; Niazy, N. N.; Das, S.; Surendran, G.; Covington, J. B. *Proc. SPIE−Int. Soc. Opt. Eng.* **1991**, *1466*, 26−38.
(8) Allen, R. D.; Opitz, J.; Larson, C. E.; Dipietro, R. A.; Breyta, G.; Hofer, D. C. *Polym. Mater. Sci. Eng.* **1997**, *77*, 451−452.
(9) Shirai, M.; Suyama, K.; Tsunooka, M. *Trends Photochem. Photobiol.* **1999**, *5*, 169−185.
(10) Thackeray, J. W.; Adams, T.; Cronin, M. F.; Denison, M.; Fedynyshyn, T. H.; Georger, J.; Mori, J. M.; Orsula, G. W.; Sinta, R. *J. Photopolym. Sci. Technol.* **1994**, *7*, 619−630.
(11) Ashmore, P. G., Dainton, F. S., Sugden, T. M., Eds.; *Photochemistry and Reaction Kinetics*; Cambridge Univ. Press: New York, 1967.
(12) Christophorou, L. G. *Atomic and Molecular Radiation Physics*; Wiley-Interscience: New York, 1971.
(13) Allen, R. D.; Optiz, J.; Larson, C. E.; Wallow, T. I.; Dipietro, R. A.; Breyta, G.; Sooriyakumaran, R.; Hofer, D. C. *J. Photopolym. Sci. Technol.* **1997**, *10*, 503−510.
(14) Cameron, J. F.; Ablaza, S. L.; Xu, G.; Yueh, W. *Polym. Mater. Sci. Eng.* **1999**, *81*, 45−46.
(15) Houlihan, F. M.; Dabbagh, G.; Rushkin, I.; Hutton, R.; Osei, D.; Sousa, J.; Bolan, K.; Nalamasu, O.; Reichmanis, E.; Yan, Z.; Reiser, A. *Chem. Mater.* **2000**, *12*, 3516−3524.
(16) McKean, D. R.; Schaedeli, U.; MacDonald, S. A. *Polym. Mater. Sci. Eng.* **1989**, *60*, 45−48.
(17) Cameron, J. F.; Orellana, A. J.; Rajaratnam, M. M.; Sinta, R. F. *Proc. SPIE−Int. Soc. Opt. Eng.* **1996**, *2724*, 261−272.
(18) Buhr, G.; Dammel, R.; Lindley, C. R. *Polym. Mater. Sci. Eng.* **1989**, *61*, 269−277.
(19) Thackeray, J. W.; Denison, M. D.; Fedynyshyn, T. H.; Kang, D.; Sinta, R. *ACS Symp. Ser.* **1995**, *614*, 110−123.
(20) Dentinger, P. M.; Lu, B.; Taylor, J. W.; Bukofsky, S. J.; Feke, G. D.; Hessman, D.; Grober, R. D. *J. Vac. Sci. Technol., B* **1998**, *16*, 3767−3772.
(21) Bukofsky, S. J.; Feke, G. D.; Wu, Q.; Grober, R. D.; Dentinger, P. M.; Taylor, J. W. *Appl. Phys. Lett.* **1998**, *73*, 408−410.
(22) Pohlers, G.; Scaiano, J. C.; Sinta, R. *Chem. Mater.* **1997**, *9*, 3222−3230.
(23) Eckert, A. R.; Moreau, W. M. *Proc. SPIE−Int. Soc. Opt. Eng.* **1997**, *3049*, 879−887.
(24) Pohlers, G.; Virdee, S.; Scaiano, J. C.; Sinta, R. *Chem. Mater.* **1996**, *8*, 2654−2658.
(25) Cameron, J. F.; Mori, J. M.; Zydowsky, T. M.; Kang, D.; Sinta, R.; King, M.; Scaiano, J.; Pohlers, G.; Virdee, S.; Connolly, T. *Proc. SPIE−Int. Soc. Opt. Eng.* **1998**, *3333*, 680−691.

acid generated by exposure can be calculated for any exposure dose as a function of depth into the resist film.

Previously, this standard addition technique was used to qualitatively illustrate that photoacid generation under deep ultraviolet exposure differs from that of the vacuum-ultraviolet and ionizing forms of radiation.[26−28] Additionally, this technique was compared to spectrophotometric titration with tetrabromophenol blue sodium salt and Rhodamine B base upon deep ultraviolet exposure.[29] Results acquired by the standard addition technique were within the variation between the results obtained using the two dyes. The technique as used in the previous studies was limited in two respects. First, the original model proposed for the technique incorporated a linear approximation for the exponential dependence of acid generated during exposure. This approximation is only valid at very small conversions of PAG to acid. Second, the concentration range of base quencher added to the resist was only 10% of the initial PAG concentration. Because of this small range, the model parameter estimates contained significant uncertainty as was evident by poor confidence intervals for the results.

In this work, we have improved both the model and the experimental method for quantifying photoacid generation by this technique. Herein we derive the relationship between the quantum yield of the photochemical reaction and the resist *C* parameter. The improved model is not limited by a linear approximation and includes the effects of strong absorption. Using the model, the resist *C* parameter was calculated for a resist system consisting of the PAG norbornene dicarboximidyl triflate (ND-Tf) in a poly(*p*-*t*-butoxycarbonyloxystyrene-*co*-*p*-hydroxystyrene) (APEX-type) resin under X-ray exposure. Significant improvement was obtained in the confidence intervals for the parameter estimates by increasing the range of base quencher to 25% of the initial PAG concentration. We tested the major assumptions involved in using resist dissolution as our analytical detection device. Through a combination of infrared and dissolution rate analysis we proved that the bulk dissolution rate dependence on the extent of deprotection of the resin polymer remains constant for base loadings as large as 25% of the initial PAG concentration. The induction effects during dissolution were also shown to be identical for resists with and without base quencher. We further justified the assumption the same extent of polymer deprotection occurs when the free acid concentration is the same for resists containing base. On the basis of these results, the standard addition technique successfully applies resist dissolution as an indirect method for quantifying photoacid generation in chemically amplified resist.

Experimental Section

A. Materials. An APEX-type resin polymer, composed of poly(*p*-hydroxystyrene) partially blocked with *tert*-butoxycarbonyl (tBOC) protecting groups, was obtained from Shipley Company. The photoacid generator, norbornene dicarboximidyl triflate (ND-Tf), was also obtained from Shipley Company. The base quencher, 1-piperidineethanol, was purchased from Aldrich Chemical Co. and used as received. Photoresist solutions were formulated by weight from solutions of individual components in propylene glycol monomethyl ether acetate (PGMEA). The concentration of PAG was 80 μmol of PAG/g of solids for each resist solution. A dilute solution of base quencher was added to solutions containing PAG and polymer to generate a series of resists containing base quencher in the range 0−25% of the molar concentration of PAG (0 to 0.25 base to PAG molar ratio). The solvent content was controlled to bring each solution in the series to a solids content of 18 wt %.

B. Sample Preparation. For all experiments except infrared analysis, 4 in. silicon wafers were primed with hexamethyldisilazane (HMDS) in a vacuum oven (Yield Engineering Systems) before resist application. Photoresist films for FTIR analysis were coated on 4 in., high-resistivity (undoped) silicon wafers without HMDS priming. Resist films were spin-cast from solution on a resist spinner (Solitec) and baked on a vacuum hot plate (Silicon Valley Group 8600 track) at 90 °C for 60 s. All resist films were prepared within 4 h of formulation to avoid possible changes in the resist performance over time. Film thickness was measured using a Nanospec AFT 215 (Nanometrics) microscope. The initial thickness of all the resist films was 800 ± 15 nm.

Exposure to X-rays was performed using the ES-1 beamline on the Aladdin electron storage ring at the Synchrotron Radiation Center at the University of Wisconsin. The X-ray spectra through the beamline and 75 μm beryllium filter was calculated to have an average energy of 2516 eV using the TRANSMIT software application offered by the Center for NanoTechnology.[30] All exposures were performed in a vacuum at less than 30 mTorr of nitrogen and without a mask (open frame). Exposure times were automatically corrected for attenuation of the beam current in the ring and converted to exposure dose values (mJ/cm^2) using flux constants determined by calorimetry. After exposure, resist wafers were baked on a vacuum hot plate (Silicon Valley Group 8600 track) at 90 °C for 90 s. The delay from exposure to the bake was minimized to less than 7 min. Samples were developed with LDD26W developer (Shipley Company, 0.26 N aqueous tetramethylammonium hydroxide) in a crystallizing dish or the dissolution rate monitor.

C. Dissolution Rates of Exposed Photoresist Films. Exposed resist samples were prepared for dissolution rate analysis by exposing 2−5 regions across the axis of a wafer, such as could be simultaneously measured with the dissolution rate monitor 5900 (Perkin-Elmer) during immersion in LDD26W developer solution. The DREAMS software was used to calculate resist thickness as a function of development time. The bulk dissolution rate was taken by a linear fit to the data at half thickness. The induction time was taken at the break between the initial slow dissolution and bulk dissolution behavior.

D. Infrared Spectra for Exposed Resist Films. Wafers used for infrared analysis were not developed after the postexposure bake (PEB). Infrared reflectance spectra were recorded for each of the 25 exposed regions from 650 to 4000 cm^{-1} using the Film Expert FTIR reflectometry workstation (On-Line Technologies) with a background reference to bare, undoped silicon. Spectra were collected at a resolution of 16 cm^{-1} and averaged over 128 scans. After spectral acquisition, each spectrum was analyzed using the Film Expert software to determine the dielectric function of the resist film. The use of undoped silicon as a reference and substrate for the infrared

(26) Pawloski, A. R.; Szmanda, C. R.; Nealey, P. F. *Proc. SPIE—Int. Soc. Opt. Eng.* **2001**, *4345*.

(27) Szmanda, C. R.; Brainard, R. L.; Mackevich, J. F.; Awaji, A.; Tanaka, T.; Yamada, Y.; Bohland, J.; Tedesco, S.; Dal'Zotto, B.; Bruenger, W.; Torkler, M.; Fallmann, W.; Loeschner, H.; Kaesmaier, R.; Nealey, P. M.; Pawloski, A. R. *J. Vac. Sci. Technol., B* **1999**, *17*, 3356−3361.

(28) Szmanda, C. R.; Kavanagh, R. J.; Bohland, J. R.; Cameron, J. F.; Trefonas, P. III.; Blacksmith, R. F. *Proc. SPIE—Int. Soc. Opt. Eng.* **1999**, *3678*, 857−866.

(29) Cameron, J. F.; Fradkin, L.; Moore, K.; Pohlers, G. *Proc. SPIE—Int. Soc. Opt. Eng.* **2000**, *3999*, 190−203.

(30) Cerrina, F.; Baszler, F.; Turner, S.; Khan, M. *Microelectron. Eng.* **1993**, *21*, 103−106.

analysis is imperative to the technique. Since the theoretical reflectivity of undoped silicon is known, the Film Expert software can simultaneously calculate the film thickness and optical constants (n and k) that fit the recorded spectrum. In this manner, reflectivity spectra were converted into the dielectric function (absorbance) using a range of Lorentzian oscillators.

Model Development

A. Description of the Photochemical Reaction. Under continuous illumination the photolysis of the PAG, P, in photoresist to generate photoacid, A, is modeled as a single reaction according to

$$\mathrm{P} \xrightarrow{h\nu} \mathrm{A} + \text{other products} \tag{1}$$

The quantum yield, ϕ, for this photochemical reaction is defined as the number of photoacid molecules generated per photon absorbed by the PAG. For this reaction, the rate of disappearance of PAG is equal to the product of the quantum yield and the photon absorption rate I_a (mJ/(cm^3 s)) as

$$\frac{\mathrm{d}P(x,t)}{\mathrm{d}t} = -\phi I_a(x,t) \tag{2}$$

where P (μmol/g) is the concentration of PAG in the resist film and t (s) is the exposure time. Since the reaction occurs within a resist film where absorption of incident radiation may occur, the concentration of PAG during exposure is a function of the depth into the film, x (μm). The intensity of light at any position in the film is described using the Beer−Lambert law by

$$I(x,t) = I_0 \exp[-\sum_{i=1}^{n} \epsilon_i \int_0^x C_i(x',t')\, \mathrm{d}x'] \tag{3}$$

where I_0 (mW/cm^2) is the time invariant source intensity incident to the surface of the film, $C_i(x,t)$ (mol/cm^3) is the time- and position-dependent concentration of species i in the resist film, and ϵ_i (cm^2/mol) is the molar absorptivity of each component. The photon absorption rate is equal to the total number of photons (energy) absorbed by the PAG per unit volume per unit time.[31] Its instantaneous value is determined from the derivative of the light intensity as

$$I_a(x,t) = -\frac{\mathrm{d}I(x,t)}{\mathrm{d}x} = \epsilon_P P(x,t) I_0 \exp[-\epsilon_P \int_0^x P(x',t')\, \mathrm{d}x'] \tag{4}$$

In most chemically amplified resist systems the absorbance of the resist film does not change during exposure; i.e., the PAG and other resist components do not photobleach.[16] The attenuation of radiation through the resist film is then independent of the concentration of PAG remaining during exposure. The intensity loss due to the absorption of light by the PAG may then be simplified using the initial PAG concentration, P_0 (μmol/g), to obtain the rate of photolysis of PAG given by

$$\frac{\mathrm{d}P(x,t)}{\mathrm{d}t} = -\phi \epsilon_P P(x,t) I_0 \mathrm{e}^{-\epsilon_P P_0 x} \tag{5}$$

Equation 5 provides the theoretical basis for determining the quantum yield for photolysis of PAG in chemically amplified resist; however, this approach has not been the traditional route for photoresist modeling. From the early work by Dill et al., the photochemical reaction has been described by[32]

$$\frac{\mathrm{d}P(x,t)}{\mathrm{d}t} = -CP(x,t)\, I(x,t) \tag{6}$$

Using the Beer−Lambert law for a constant intensity source and a nonbleaching resist film, the intensity of light in the film is described by

$$\frac{\mathrm{d}P(x,t)}{\mathrm{d}t} = -CP(x,t) I_0 \mathrm{e}^{-\alpha x} \tag{7}$$

where α (μm^{-1}) is the total absorption coefficient for the film. The quantum yield and the C parameter from eqs 5 and 7 differ in their basis for photon absorption by the resist. Equation 5 considers only the photons absorbed directly by the PAG, while the entire intensity function through the resist is used in eq 7. The C parameter contains all the fundamental information on the quantum yield; however, its value is based on the total energy deposited within the resist film. Matrix effects in a condensed phase may alter the efficiency of a photochemical reaction due to complex energy transfer mechanisms.[11,12] Furthermore, under exposure to ionizing radiation the radiation chemistry of the resist is predominantly due to the generation of Auger electrons.[33] Since the matrix resin is present in the largest concentration, the majority of Auger electrons originate from the resin polymer and not the PAG. For these reasons it is generally preferred to characterize photoacid generation by the C parameter instead of the quantum yield, and the model derived below follows this formalization.

B. The Average Acid Concentration for Resists Containing Base Quenchers. The concentration of PAG in the resist film after exposure may be written as

$$P(x,t) = P_0 \exp\{-CtI_0 \mathrm{e}^{-\alpha x}\} \tag{8}$$

after integration of eq 7. The product of the exposure time and the intensity of radiation incident to the surface is equal to the exposure dose, D_0 (mJ/cm^2), at the resist surface.[34] The use of exposure dose to replace exposure time is preferred in resist characterization since it describes the amount of energy applied to the resist per area. Equation 8 may now be written as

$$P(x,D_0) = P_0 \exp\{-CD_0 \mathrm{e}^{-\alpha x}\} \tag{9}$$

(31) Calvert, J. G.; Pitts, J. N. *Photochemistry*; Wiley: New York, 1966.

(32) Dill, F. H.; Hornberger, W. P.; Hauge, P. S.; Shaw, J. M. *IEEE Trans. Electron Devices* **1975**, *ED22*, 445−452.

(33) Anderson, D. W. *Absorption of Ionizing Radiation*; University Park Press: Baltimore, 1984.

(34) The exposure dose is equal to the integral of the exposure intensity over the illumination time. However, the source intensity is constant for this case, and the exposure dose is equal to the product of the intensity and exposure time.

to relate the photogenerated acid concentration anywhere within the film as a function of the exposure dose delivered to the surface of the resist.

For every molecule of PAG decomposed during exposure it is assumed that one molecule of acid is generated. The photogenerated acid concentration, A_{Gen}, is related to the PAG concentration by

$$A_{Gen}(x,D_0) = P_0 - P(x,D_0) \quad (10)$$

Substitution and simplification gives

$$A_{Gen}(x,D_0) = P_0(1 - \exp\{-CD_0e^{-\alpha x}\}) \quad (11)$$

The average concentration of photogenerated acid is then determined by

$$\langle A_{Gen}\rangle = \frac{P_0}{x_0}\int_0^{x_0} 1 - \exp\{-CD_0e^{-\alpha x}\}\, dx \quad (12)$$

where x_0 is thickness of the resist film. By a substitution of variables for $CD_0e^{-\alpha x}$ the integral in eq 12 may be solved in terms of the exponential integral function, defined by

$$E_i(x) = \int_x^{\infty}\frac{e^{-u}}{u}\, du \quad (13)$$

to obtain the solution

$$\langle A_{Gen}\rangle = \frac{P_0}{\alpha x_0}[E_i(-CD_0e^{-\alpha x_0}) - E_i(-CD_0)] + P_0 \quad (14)$$

To determine the value of the C parameter from eq 14 would require direct measurement of the photogenerated acid concentration. These measurements are difficult and laborious to perform in thin films of resist. To circumvent this issue, base quenchers are used to indirectly determine acid concentration in a manner similar to a standard addition experiment.

For resist films loaded with a uniform concentration of base quencher, B (μmol/g), the neutralization of photogenerated acid is assumed to be fast and complete. Recent development of the proportional neutralization model has shown that acid is neutralized by a stoichiometric amount of base immediately after exposure and does not depend on the postexposure bake.[35,36] After neutralization has occurred the free acid concentration, A_{Free}, in the resist film is given by

$$\langle A_{Free}\rangle = \langle A_{Gen}\rangle - B \quad (15)$$

$$\langle A_{Free}\rangle = \frac{P_0}{\alpha x_0}[E_i(-CD_0e^{-\alpha x_0}) - E_i(-CD_0)] + P_0 - B \quad (16)$$

The development of positive tone photoresist films in aqueous base is governed by the extent of removal of blocking groups during the PEB, and that process depends on the amount of acid within the resist film. Adding base to the resist requires an increase in the exposure dose to achieve the same degree of polymer deprotection since additional acid must be generated to overcome neutralization by the base. We assume that the same degree of deprotection is reached for a given free acid concentration when all processing conditions remain constant. Since resist dissolution is governed by the removal of protecting groups, we can further assume that equal dissolution rates are obtained for resist films containing the same free acid concentration. These assumptions have been justified for the resist system used in this work and will be discussed later.

To implement the technique, resist dissolution is used as an indirect method for detecting equivalent free acid concentrations. The exposure dose that produces the same dissolution rate is experimentally determined for a series of resist formulations containing base. Although the acid concentration to achieve this dissolution rate is not known, we assume that it is the same for each resist. Equation 16 may then be simultaneously solved for the free acid concentration and the C parameter by nonlinear minimization to the experimental data (D_0 vs B).

Results and Discussion

A. Calculation of the *C* Parameter and Free Acid Concentration. Resist films were prepared from solutions containing ND-Tf and 1-piperidineethanol in an APEX-type resin. All processing conditions were identical for every sample. The molar ratio of 1-piperidineethanol to the initial PAG concentration ranged from 0 to 0.25. Each film was exposed to increasing doses of X-ray radiation across 25 open field exposure zones.[37] After the PEB (90 °C, 90 s), each film was developed in aqueous base for 20 s. The remaining resist thickness was measured for each exposure zone and normalized to the remaining thickness of the unexposed regions. Figure 1 shows representative contrast curves (normalized remaining thickness (NRT) vs exposure dose) for various base loadings. As the base quencher concentration increases, the exposure dose required to develop the film is pushed to higher values of dose. From each contrast curve, the dose to completely develop each resist film (dose to clear) was recorded for each concentration of added base. The initial thickness of all the resist films was 800 ± 15 nm, and a film absorption coefficient of 0.022 μm^{-1} was calculated by atomic scattering cross sections.[38,39]

The parameters A_{Free} and C were calculated using eq 16 and a nonlinear fitting routine in Mathmatica (Wolfram Research). Experimental data and the model prediction are shown in Figure 2. Error bars represent

(35) Hinsberg, W. D.; Houle, F. A.; Sanchez, M. I.; Morrison, M. E.; Wallraff, G. M.; Larson, C. E.; Hoffnagle, J. A.; Brock, P. J.; Breyta, G. *Proc. SPIE—Int. Soc. Opt. Eng.* **2000**, *3999*, 148−160.

(36) Hinsberg, W.; Hoffnagle, J.; Houle, F. *Solid State Technol.* **2000**, *43*, 95−96, 98, 100, 102.

(37) X-ray radiation was used as a model exposure source for ionizing forms of radiation that have been targeted for sub-100 nm lithography (EUV and e-beam). X-ray exposures allow for much thicker resist films than for EUV exposures due to absorbance issues. The X-ray exposure system also permits very large exposure fields that are not possible for e-beam systems. Although thick films and large exposed regions are not necessary for the standard addition technique, they are necessary to perform dissolution and infrared analysis of exposed resist films.

(38) The absorption coefficient at 2516 eV was calculated on the basis of the atomic composition of the resin polymer and the photoacid generator, assuming a density of 1.15 g/cm^3.

(39) Henke, B. L.; Gullikson, E. M.; Davis, J. C. *At. Data Nucl. Data Tables* **1993**, *54*, 181−342.

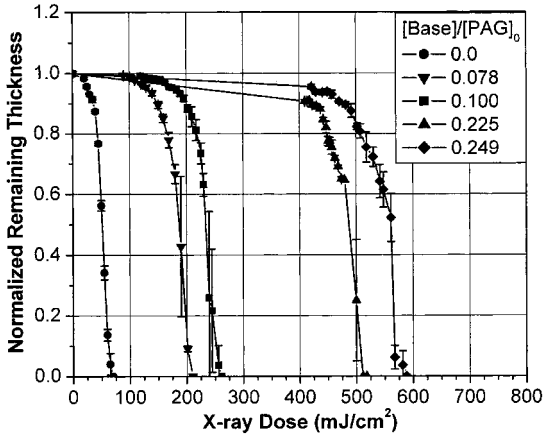

Figure 1. Typical resist contrast curves for the ND-Tf/APEX resist system containing increasing concentration of the base quencher, 1-piperidineethanol. Addition of base increases the exposure dose required to develop the resist film. From these curves, the dose to clear the resist film is recorded for each concentration of base quencher.

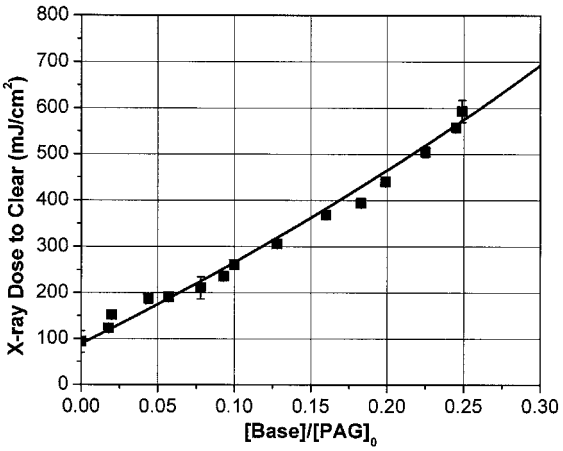

Figure 2. Experimental data and model predictions for the dose to clear dependence on the concentration of base quencher. Data points mark the dose to clear value measured from contrast curves. Error bars are representative of the standard deviation of multiple measurements and usually are within the step size of the incremental exposures. Equation 16 is used for nonlinear minimization to the experimental data to determine the resist *C* parameter and free acid concentration.

the standard deviation of multiple measurements and were used for weighting the error during minimization. For the ND-Tf/APEX system the *C* parameter is calculated as 0.000 64 cm^2/mJ with a free acid concentration of 4.4 μmol/g (0.055 acid/PAG_0 ratio). The 95% confidence intervals for the calculation are 0.000 59−0.000 68 cm^2/mJ and 3.5−5.3 μmol/g for the *C* parameter and free acid concentration, respectively.

In previous work, the maximum concentration of base added to the resist was only 10% of the initial PAG concentration.[26,27,29] By extending the range of the base quencher to 25% of the PAG concentration, the confidence intervals of the estimated parameters have been greatly improved. For example, repeating the calculation in this work including only the data up to 10% of the PAG concentration yields a *C* parameter estimate of 0.000 72 cm^2/mJ with a 95% confidence interval of 0.000 54−0.000 89 cm^2/mJ. The range of the confidence interval has been improved from approximately 48% to 14% of the value of the estimated parameter. The

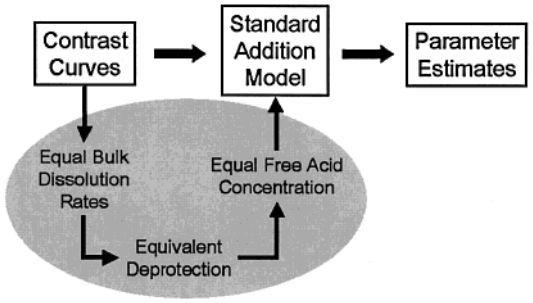

Figure 3. Schematic representation of the assumptions behind the application of experimentally measured contrast curves to estimate parameters that describe the exposure chemistry of photoresist using the standard addition model.

increase in certainty of the parameter estimation is important for discerning small differences between similar photoresist systems.

B. Resist Dissolution May Be Used as an Analytical Detector for Determining Equivalent Free Acid Concentrations. A key assumption of the standard addition technique, described and implemented above, was that the base quencher acted only to neutralize a stoichiometric amount of acid. It is possible that the base quencher could also alter resist properties by plasticization, variation of the deprotection kinetics, alteration of diffusive properties, further radiation chemistry, incomplete neutralization, or additional acid−base chemistry within the resist or during development. If any of these processes exist, then the validity of the technique is in question. We were unable to investigate each possible complication individually, but we were able to justify the desired end result that resist dissolution may be used as an analytical tool to indicate equivalent free acid concentrations in exposed resist films.

We considered the assumptions that connect resist dissolution as an analytical detector to the model used for parameter estimation. Figure 3 graphically illustrates these issues. First, we verified that the dependence of the bulk dissolution rate on the extent of removal of protecting groups remains the same when base quencher is added to the resist. Next, we showed that the induction effects present during resist dissolution are the same for resists with and without base. This verified that data taken from contrast curves at a given developed thickness or dose to clear are representative of equivalent bulk dissolution rates. To connect equivalent dissolution rates to equivalent free acid concentrations required by the model, we demonstrated that the same free acid concentration produced within each resist film leads to the same removal of protecting groups from the resin polymer. By considering these three issues, we have validated the methodology of the standard addition technique.

1. Resist Dissolution Dependence on Deprotection Remains Constant for Increasing Base Concentration. The following analysis showed that the dissolution rate of resists containing different amounts of base quencher depends only on the extent of resin deprotection. The bulk dissolution rate for exposed resist films loaded with base quencher is illustrated in Figure 4. The data were fit to the equation

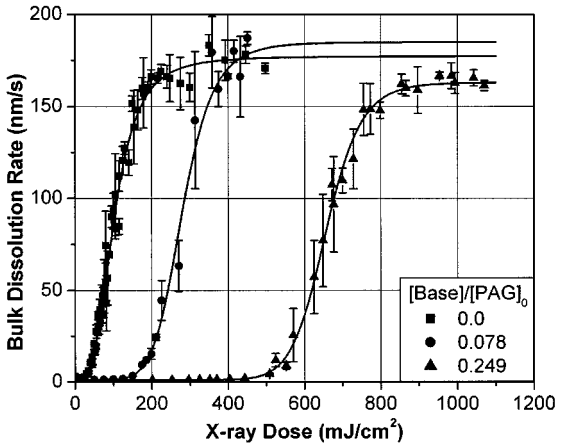

Figure 4. Bulk dissolution rates for resist films exposed to X-ray radiation as determined by a dissolution rate monitor. The bulk dissolution rate is determined at half the resist thickness. Error bars represent the standard deviation of multiple measurements. The solid lines are a least-squares fit of the data to eq 17 using error bar weighting.

$$y = \frac{A_1 - A_2}{1 + (x/x_0)^p} + A_2 \qquad (17)$$

using Origin6.1 (OriginLab) software, where A_1 and A_2 are the minimum and maximum dissolution rates, x_0 is the exposure dose at the center of the curvature, and p is the power dependence. Each set of data was fit independently using error bar weighting and constraining the lower bound to a value greater than or equal to zero. The parameters in eq 17 do not represent a physical interpretation of the dissolution behavior of resists and are only used to represent the collected data. The difference between the curves is consistent with acid neutralization by the base quencher.

For the same formulations, infrared spectra were recorded for exposed films. Two bond stretching regions characteristic of the tBOC protecting group located at 1149 cm^{-1} (ester, C−O−C) and 1735 cm^{-1} (carbonyl, C═O) were monitored to evaluate the relative extent of polymer deprotection. During our analysis both regions were analyzed, and both were found to produce nearly identical results. Figure 5 displays the infrared absorbance measured at 1149 cm^{-1} as a function of exposure dose. Consistent with other studies, the infrared absorbance does not reach zero despite large exposure doses.[40,41] Error bars represent the standard deviation of multiple measurements at each exposure zone.

The decrease in infrared absorption is proportional to the number of protecting groups removed from the matrix resin by acid catalysis during the PEB. The dependence of the resist dissolution rate on the coverage of protecting groups was obtained by combining both the dissolution rate and infrared data. For each exposure dose at which an infrared spectrum was recorded, the dissolution rate was calculated using the fit to eq 17. In this respect, a universal curve for the resist dissolution rate dependence on the extent of deprotection was generated, as shown in Figure 6. This universal curve illustrates that the dependence of the bulk dissolution rate on the extent of resin deprotection remains constant for loadings of 1-piperidineethanol as large as 20 μmol/g.

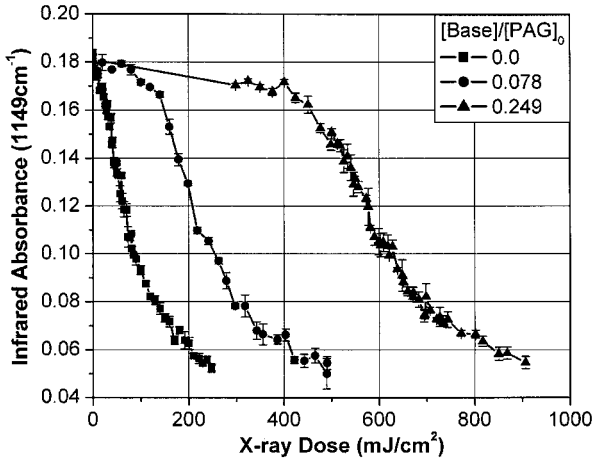

Figure 5. Infrared absorbance at 1149 cm^{-1} for resist films exposed to X-ray radiation. Error bars represent the standard deviation of three measurements in each exposure zone. Infrared spectra for samples containing base ratios of 0.0 and 0.249 were taken from two independent samples for each base concentration, indicating excellent reproducibility of the measurements.

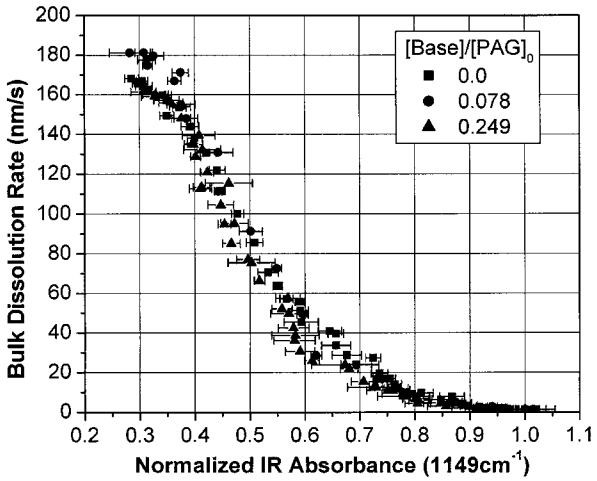

Figure 6. Universal curve for resist dissolution rate dependence on the remaining coverage of protecting groups. The data from Figures 4 and 5 are combined by calculating the dissolution rate for each exposure dose that an infrared spectrum has been recorded. Error bars have been included from the infrared absorbance, but no estimate of error from the calculation was made.

2. Dissolution Induction Effects are Independent of Base Addition. The standard addition technique uses contrast curves as an approximation of the true dissolution rate behavior of resist films. For the technique, we arbitrarily chose a value for thickness loss and measured the dose required to develop that thickness of resist. The dose to clear the entire film was used in this study for simplicity. Resist dissolution is often accompanied by induction effects near the surface of the resist film, and the initial dissolution of the film may be significantly slower than the bulk.[42] The magnitude of these effects is not necessarily constant for a given resist system and can vary with the amount of exposure

(40) Ito, H.; Sherwood, M. *J. Photopolym. Sci. Technol.* **1999**, *12*, 625−636.
(41) Thackeray, J.; Fedynyshyn, T. H.; Kang, D.; Rajaratnam, M. M.; Wallraff, G.; Opitz, J.; Hofer, D. *J. Vac. Sci. Technol., B* **1996**, *14*, 4267−4271.

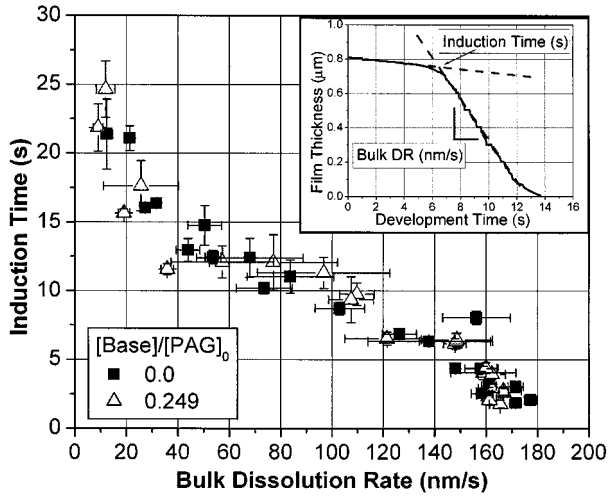

Figure 7. Dependence of the induction time during resist dissolution on the bulk dissolution rate. Error bars show the standard deviation of multiple measurements. Inset: The induction time is taken at the break between the initial and bulk dissolution behavior.

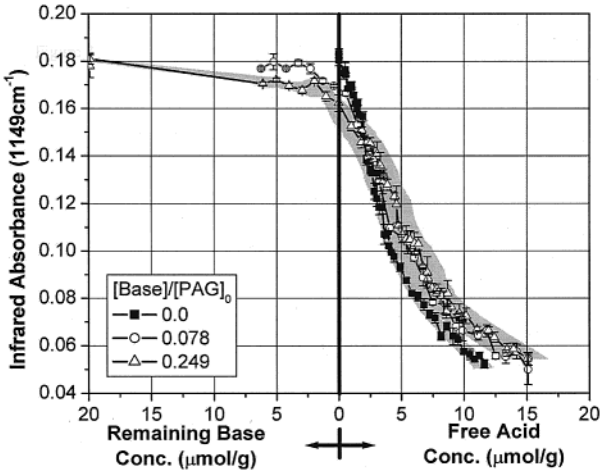

Figure 8. Infrared absorbance as a function of the acid and base concentration within the resist film. The decrease in infrared absorbance is proportional to the extent of polymer deprotection. The concentration of acid is calculated using the *C* parameter determined from contrast curves for this resist system. Values to the left of zero indicate that the exposure has not generated enough acid to neutralize all the base added to the resist. Values to the right of zero indicate the concentration of free acid in the film after neutralization. The shaded region represents the variation in the calculation of the free acid concentration by implementing the 95% confidence intervals for the *C* parameter and smoothing the calculated values.

delivered to the film, presumably due to the creation of acid and subsequent deprotection of the resin. Because of these induction effects, the average dissolution rate calculated from contrast curves by dividing the developed thickness by the development time does not necessarily agree with the bulk dissolution rate of the film measured by a dissolution rate monitor. Accordingly, these discrepancies are larger for short development times and thinner resist films.

As long as the addition of base to the resist does not alter the induction effects, the substitution of contrast curves for true dissolution behavior is valid. We measured the induction time from the raw data obtained by the dissolution rate monitor. As shown in Figure 7, the induction time is plotted against the bulk dissolution rate of the film for systems containing 0.0 and 0.249 ratio of base to initial PAG loading. The induction time was taken at the break between the initial and bulk dissolution behavior as shown in the inset of Figure 7. For conditions at which the bulk dissolution rate is the same for films with and without base, the induction time is likewise equal. Since both the induction times and the bulk dissolution rates are equal, the amount of resist removed during a timed development will also be equal. Therefore, contrast curves may be used for this system to mark equivalent bulk dissolution behavior.

3. Same Deprotection for Equal Free Acid Concentrations. To verify that the same free acid concentration produced in each resist of the series removed an equivalent number of protecting groups during the PEB, we again employed the measurements of infrared absorbance from Figure 5. Using eq 16 and the *C* parameter determined above, infrared absorbance was plotted as a function of the calculated free acid concentration present in the film, as shown in Figure 8. A value of zero on the *x*-axis denotes no acid or base present in the film. Values to the left of zero indicate base remaining in the film, and values to the right of zero represent the free acid concentration. The shaded region represents the uncertainty of the calculation for resists containing a base to PAG ratio of 0 and 0.249 and was obtained by repeating the calculation using the 95% confidence interval for the *C* parameter. The data sets for these two formulations agree within the confidence of the parameter estimation.

Since the extent of resin deprotection is proportional to the infrared absorbance at 1149 cm^{-1}, Figure 8 shows how deprotection depends on the free acid concentration in the film. Resist films containing base seem to exhibit a small degree of deprotection before complete neutralization of the base (*x*-axis value of zero). The effect appears to become more problematic as the base concentration increases. It is possible that the neutralization reaction does not go to completion before the PEB, as was assumed by the proportional neutralization model.[35,36] Another possibility is the breakup of the acid−base complex during baking, releasing some of the free acid. This small amount of residual acid may catalyze deprotection reactions during the PEB before it is quenched by base. The consequence would be an overestimate of the *C* parameter, and larger errors would incur for resist systems or conditions where the extent of deprotection needed to develop the film is very small. Although this observation does not support any definitive conclusions, it may indicate that the proportional neutralization model is limited to a concentration range of base. In contrast, the confidence intervals obtained during parameter estimation are improved by extending the base concentration. For the ND-Tf/APEX/1-piperidineethanol system, a maximum base ratio of 0.25 appeared to satisfy the tradeoff between these effects. Within this range of base the dependence of resist deprotection on the free acid concentration is the

(42) Flanagin, L. W.; Singh, V. K.; Willson, C. G. *J. Polym. Sci., Part B: Polym. Phys.* **1999**, *37*, 2103−2113.

same for every resist. Therefore, it is reasonable to assume that an equivalent removal of blocking groups occurs from the same free acid concentration.

Conclusions

We have described and validated a technique to quantify photoacid generation in chemically amplified photoresist. The standard addition method is essentially applicable to all chemically amplified resist platforms; however, the following consideration should be applied to the selection of the base quencher. The base quencher must be a strong base, soluble in organic solvents, miscible and stable in photoresist solutions, and soluble in aqueous base developer. Bases of low volatility are also preferable to minimize chance of evaporation during thermal processing, and most importantly, the base quencher should not inhibit the dissolution of the resist in aqueous base. For the system studied, 1-piperidineethanol appeared to meet all these criteria since the resist dissolution dependence on the removal of protecting groups remained constant. Other base quenchers should similarly be characterized before applying them to the technique.

It is extremely important to maintain constant processing conditions for each of the resists in the series. The post-apply bake, exposure, postexposure bake, and development conditions must all be performed with rigorous attention to reproducibility. Likewise, each resist film must be cast to achieve the same initial film thickness. As long as each resist film in the series is processed under identical conditions, all processing variables are removed from the effects of the radiation chemistry. Similarly, adjusting the PEB or development conditions for the entire series should not alter the determination of the C parameter; however, the value of the free acid concentration under the new conditions will not be the same. Further work is required to verify that the model predicts the same C parameter when processing conditions are varied.

The standard addition technique is advantageous over other techniques since it does not require additional processing equipment or procedures other than those found in most wafer processing laboratories. Resist films are processed under realistic conditions generating results entirely applicable to parameters required in photoresist simulation packages. In addition, this technique does not require large areas of exposed resist, allowing photoacid efficiency to be determined for all forms of radiation including electron beam writing, for example, that has previously been excluded by practicality. This new technique offers exciting opportunities to explore the differences of photoacid generation across all exposure platforms, increasing our understanding of resist chemistry and aiding in the development of the next generation of resists.

Acknowledgment. The authors express gratitude to the following individuals for their assistance and discussions during our continuing work: Charles Szmanda, James Rawlings, David Medeiros, Leo Ocola, Franco Cerrina, Sylvie Bosch-Charpaney, Frank Houlihan, James Cameron, Ranjeet Tate, and Juan de Pablo. Gratitude is also expressed to the Semiconductor Research Corporation for their funding through the Graduate Fellowship program. This work is based in part by a grant from the Semiconductor Research Corporation under Grant 98-LP-452. The Center for Nanotechnology, University of Wisconsin—Madison, is supported in part by DARPA/ONR Grant N00014-97-1-0460. The Synchrotron Radiation Center of the University of Wisconsin—Madison is supported by the National Science Foundation under Grant DMR-0084402.

CM010529A